



Contents lists available at ScienceDirect



Catalysis Today

journal homepage: www.elsevier.com/locate/cattod

Kinetic analysis and process modeling for cellulose valorization in cooperative ionic liquid pairs

Sijie Liu, Luo Tang, Jinxing Long, Jianyu Guan*, Xuehui Li*

School of Chemistry and Chemical Engineering, Pulp & Paper Engineering State Key Laboratory of China, South China University of Technology, Guangzhou 510640, PR China

ARTICLE INFO

Article history:

Received 28 May 2015

Received in revised form 21 July 2015

Accepted 23 July 2015

Available online xxx

Keywords:

Reaction kinetics

Process modeling

Ionic liquids

Catalytic degradation

Cellulose

ABSTRACT

Studies on kinetic analysis and process modeling are important and necessary for the development of novel and efficient technology for cellulose utilization. In this study, a kinetic model for the batch reactor was described for catalytic cellulose degradation in cooperative ionic liquid pairs based on an intensive analysis of the experimental parameters. Our fitting results show that the proposed model agrees well with the experimental data. The kinetic parameters obtained from the above model were subsequently applied to the continuous stirred tank reactor (CSTR) by constructing a mathematical process model for the continuous operation of cellulose degradation combined with product separation. The effects of reaction temperature, retention time, extract flow rate and distribution coefficients were intensively investigated. The numerical results demonstrate that relatively high temperature and larger retention time are favorable in cellulose conversion, whereas the product distribution coefficient and extract flow rate mainly affect the concentration of the hexane-soluble fraction (volatile chemicals). The findings presented in this work will serve as a beneficial reference for further biomass transformation of industrial purpose.

© 2015 Elsevier B.V. All rights reserved.

1. Introduction

Conversion of biomass substance to bio-fuel or chemicals is being actively pursued because of its great potential for relieving the environmental pollution and energy crisis [1]. However, typical transformation methods for this process are generally cost-ineffective due to the complex and highly recalcitrant property of the biomass composition caused by the robust 3D hydrogen bond network, so the current technologies are unable to meet the requirement of large scale commercialization [2,3]. Therefore, efficient biomass valorization technology at mild conditions is crucial and highly desirable. Catalytic liquefaction is regarded as a useful technique for biomass valorization because of its comparatively mild reaction condition (low temperature and pressure) and concentrated production distribution [4]. In general, both chemical and biochemical catalytic processes are considered to be efficient strategies for biomass liquefaction [5–8]. However, the liquefaction efficiencies are still improvable because the lignocellulosic biomass is normally non-dissolvable in both water and traditional organic solvents. Various process intensification techniques thereby have

been extensively explored for promoting the liquefaction degree, product yield and selectivity, and reducing the reaction temperature and time [9–11].

In 2002, Rogers and coworkers found that cellulose can be directly dissolved in alkyl-imidazolium ionic liquids (ILs) under a moderate condition with 10 wt% solubility [12], which opens up a new perspective for the homogeneous liquefaction of biomass and its components. ILs as a novel solvent or efficient catalyst for biomass disposition has thereby received increasing attention [13–16] and it is regarded as a useful solvent to achieve biomass valorization. For example, the efficient hydrolysis of cellulose was reported with more than 77% yield of reducing sugar over the ILs [bmim]Cl and proton acid catalyst [17]. The conversion of cellulose and real lignocellulosic biomass to fine chemicals, such as 5-hydroxymethylfurfural (HMF) and levulinic acid, were also extensively examined [18–20]. However, in most of the above-mentioned processes, cellulose should be pre-dissolved in the ILs. Therefore, the liquefaction efficiency in these processes is still an issue due to the limited solubility of biomass in ILs. In order to solve this problem, we previously proposed a dissolution and *in-situ* degradation mode for cellulose and lignocellulosic biomass liquefaction at mild conditions using cooperative IL pairs [21–23]. In a typical approach [21], the cellulose was first partially dissolved by the IL solvent to give a homogeneous medium, and then this

* Corresponding authors. Tel.: +86 20 87114707.

E-mail addresses: cejyguan@scut.edu.cn (J. Guan), cexhli@scut.edu.cn (X. Li).

Nomenclature

c_0	initial cellulose concentration in reactor (g/L)
c_c	catalyst concentration (g/L)
c_f	fast-reaction part concentration (g/L)
c_h	hexane-soluble products concentration (g/L)
c_m	methanol-soluble products concentration (g/L)
c_m^E	methanol-soluble products concentration in extract (g/L)
c_h^E	hexane-soluble products concentration in extract (g/L)
c_{rf}	active concentration of fast-reaction part (g/L)
c_{rs}	active concentration of slow-reaction part (g/L)
c_s	slow-reaction part concentration (g/L)
k	rate constant
k'	reaction constant correlated with catalyst concentration (s^{-1})
m_0	initially total cellulose mass (g)
m_{s0}	initial slow-reaction part mass (g)
R_1	distribution coefficient of methanol-soluble products
R_2	distribution coefficient of hexane-soluble products
r	reaction rate (g/sL)
r_c	cellulose degradation rate (g/sL)
S	solubility of cellulose in ILs (g/100 g ILs)
T	temperature (K)
t	time (s)
t_R	average retention time of feedstock (s)
V	volume (L)
v	mass flow rate (g/s)
ϕ	ratio of slow-reaction part
ρ	density (g/L)

Subscripts

f	fast-reaction
IL	ionic liquid
m	methanol-soluble products
h	hexane-soluble products
s	slow-reaction
1	methanol-soluble products conversion to hexane-soluble products
-1	hexane-soluble products conversion to methanol-soluble products

IL/cellulose homogenous medium was catalytically degraded to useful chemical while a coordinated acidic IL was used as catalyst simultaneously. With the synergic effect of the cooperative IL pairs (one IL serving as the solvent for cellulose dissolution and the other as the catalyst for the degradation), cellulose can be completely converted to useful industrial chemical in a single batch reaction at mild conditions (473 K for 15 min). The dragging of the dissolution equilibrium, combined with the rapid, *in situ* acid-catalyzed degradation of bulk insoluble cellulose, overcame the long intrinsic problem of cellulose insolubility encountered in the conversion of biomass to biochemical. However, as the most prominent problems in current biomass conversion processes, complex combination and optimization of process factors, such as product separation, comprehensive energy utilization, solvent recycling and realization of continuous operation are far from being resolved [3] and thus should be comprehensively understood and intensively investigated. In contrary to catalysis chemistry studies, kinetic modeling and whole process simulation are able to provide deep understanding about the optimal design of the process. Such efforts are currently still in great need [24]. Our previous dissolution

and *in situ* degradation method for the transformation of cellulose and lignocellulosic biomass was originally focused on the biomass valorization in batch reactor. Its effectiveness and efficiency in comprehensive utilization of energy, convenient separation of products and mass production of biomass need to be examined and evaluated in the industrial scope.

In this work, we proposed a reaction kinetic model for the cellulose catalytic liquefaction based on the cooperative IL pairs system. The kinetic property of the cellulose degradation in a batch reactor was first investigated and analyzed. And then, based on the parameters obtained from the batch reactor, an intensive process simulation of the continuous process for cellulose depolymerization plus the product separation in an integrated reactor was put forward to provide an insight into the industrial valorization of lignocellulosic biomass and its components.

2. Experimental

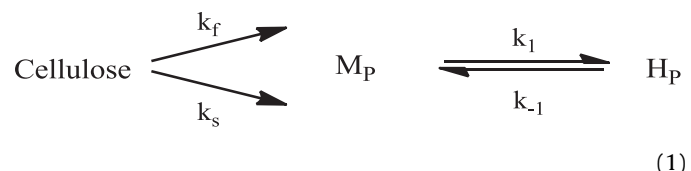
Cellulose degradation is carried out in a 150 mL stainless autoclave as a batch reactor. Typically, 5 g cellulose, designated amount of cooperative ILs (20 g bmimCl and 3.5 mmol $C_4H_8SO_3HmimHSO_4$), 10 mL methanol and 80 mL hexane are added to the reactor. After displacing the air in the reactor with nitrogen, the reactor is heated and kept at designated temperature for 15 min, and then the mixture of IL and products are cooled to room temperature for separation.

The product from the cellulose degradation forms two phases in a separating funnel, and is first separated. The heavy component fraction is then exacted by hexane for three times to remove the residual volatile chemical in the IL. By collecting the extract and the upper phase product, the hexane-soluble fraction is obtained. After a sequence of IL removal operations (extracted by CH_2Cl_2) and dilution with methanol, the nonvolatile product from the cellulose dissolution and degradation process is obtained as the methanol-soluble fraction. The volatile components are determined with a gas chromatography mass spectrometry (GC-MS). The molecular weight distribution of the methanol-soluble fraction is measured with a gel permeation chromatography (GPC) and the particle size of this fraction was measured with the Malvern analysis [21].

3. Modeling

3.1. Kinetic model in batch reactor

The dissolution and *in situ* catalytic degradation of cellulose by cooperative IL pairs are a complex process [21], in which part of the feed cellulose is dissolved by the IL solvent to yield a homogeneous solution at first, and then it can sufficiently contact with another acidic IL catalyst to form an efficient process. At the same time, the depolymerization of cellulose in the first step can be divided into two fractions: fast-reaction and slow-reaction parts to obtain the methanol-soluble products. Then, the second step about further degradation of the methanol-soluble products, as a homogeneous reaction, can be simplified as a reversible first order process. This two-step reaction model in a batch reactor is described as Eq. (1):



where M_P and H_P represent the methanol-soluble and hexane-soluble products, respectively. The rate constants k_f and k_s are for the fast reaction and slow reaction, whereas k_1 and k_{-1} denote the

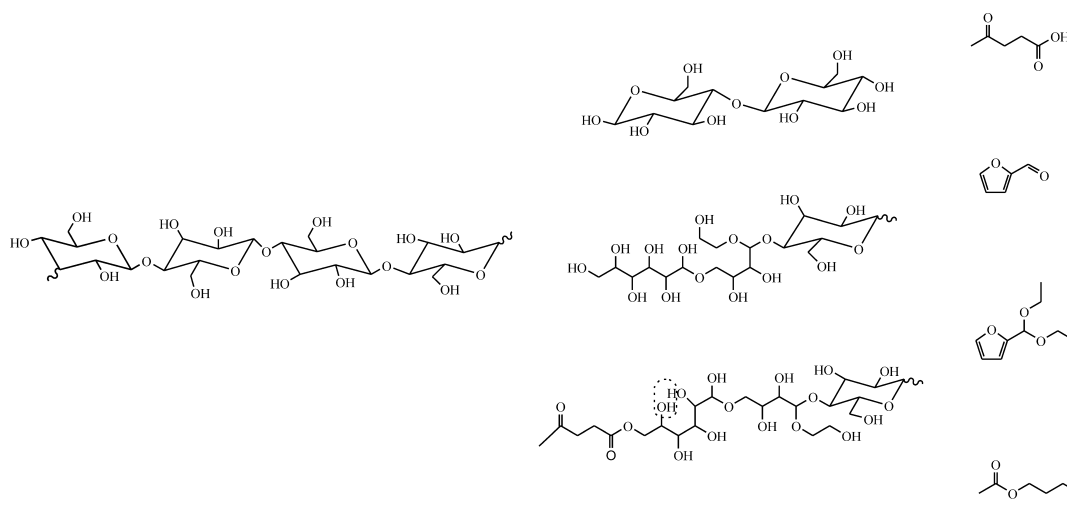


Fig. 1. Molecule structure of cellulose and its degradation products.

rate constants for the degradation of the methanol-soluble products and its reversible process.

During the degradation, the cellulose is first depolymerized to a nonvolatile oligomer (the methanol soluble fraction), and then this oligomer is further degraded to the final products, which may be extracted by hexane. Fig. 1 describes the molecule structure of cellulose and the representative degradation products. The methanol soluble fraction has a molecular weight of 788–1025 [21], which is considered to be oligomer of the products and the part degradation cellulose. The Malvern analysis demonstrates their size distribution within 20–300 nm. The lighter fractions that dissolve in the hexane are small molecule compounds such as levulinic acid, furfural, butyl acetate and 2-(diethoxymethyl)furan. All of them have a high solubility in hexane. Cellulose and all of the degradation products are dissolvable in the IL, but due to extracting by hexane and methanol, only a trace of products existed in the IL, therefore the products in the IL may be neglected in this batch reactor model.

According to this model, the kinetics of cellulose degradation can be proposed by the following power-law equations including the reaction constant, reactant concentration and catalyst concentration (Eqs. (2)–(5)).

$$r_f = \frac{dc_f}{dt} = -k_f c_c^\alpha c_f \quad (2)$$

$$r_s = \frac{dc_s}{dt} = -k_s c_c^\beta c_s \quad (3)$$

$$r_1 = \frac{dc_m}{dt} = k_f c_c^\alpha c_f + k_s c_c^\beta c_s - k_1 c_c^\gamma c_m + k_{-1} c_c^\varphi c_h \quad (4)$$

$$r_{-1} = \frac{dc_h}{dt} = k_1 c_c^\gamma c_m - k_{-1} c_c^\varphi c_h \quad (5)$$

where c_c , c_f , c_s , c_m and c_h stand for the concentration of catalyst, cellulose in fast reaction, cellulose in slow reaction, methanol-soluble products and hexane-soluble products, respectively, r is the reaction rate, and α , β , γ and φ are the corresponding exponent of the catalyst concentrations.

Generally speaking, the content of the slow-reaction cellulose is mainly dependent on the source of cellulose and the temperature [25]. Recent studies also shows that the crystallinity, which usually directly relates to the contents of the slow-reaction and fast-reaction cellulose, positively depends on the temperature [26], which is also accords well with our previous studies about the

process of biomass degradation [21–23]. Therefore, the same correlation of cellulose crystallinity and temperature is adopted to describe the ratio of the slow-reaction Φ , and the interrelation between the crystallinity and the reaction temperature T can be expressed in Eq. (6), according to the experimental data obtained under temperature of 460 K [26]. At high temperature (higher than 460 K), the value of Φ is set to be equal to zero.

$$\Phi = \frac{m_{s0}}{m_0} = -0.0153T + 7.0437, \quad (6)$$

where m_{s0} is the initial slow-reaction part mass, and m_0 is the initially total cellulose mass.

Because the detailed quantitative effect of acidic IL catalyst on this process is difficult to obtain, the influence of catalyst is assumed to be contained in the rate constants. Furthermore, taken into consideration of the feature of heterogeneous reactions, the concentration of cellulose should be adjusted in the first step of the reactions. In fact, cellulose particles are dissolved in the IL pairs prior to reacting, so the concept of an active reaction concentration that relates to the solubility is adopted. The rate equations for the batch reactor can thereby be modified and listed in Eqs. (7)–(10):

$$r_f = \frac{dc_f}{dt} = -k'_f c_{rf} \quad (7)$$

$$r_s = \frac{dc_s}{dt} = -k'_s c_{rs} \quad (8)$$

$$r_1 = \frac{dc_m}{dt} = k'_f c_{rf} + k'_s c_{rs} - k'_1 c_m + k'_{-1} c_h \quad (9)$$

$$r_{-1} = \frac{dc_h}{dt} = k'_1 c_m - k'_{-1} c_h \quad (10)$$

where k' represents the reaction constant correlated with the catalyst concentration, c_{rf} is the active concentration in the fast reaction and c_{rs} is the active concentration in the slow reaction. The value of c_{rf} and c_{rs} may be calculated as follows:

$$c_{rf} = \min \left(c_f, \frac{(1 - \Phi) S \rho_{IL}}{100} \right) \quad (11)$$

$$c_{rs} = \min \left(c_s, \frac{\Phi S \rho_{IL}}{100} \right) \quad (12)$$

where S is the solubility of cellulose in the IL pairs, and ρ_{IL} is the density of IL pairs.

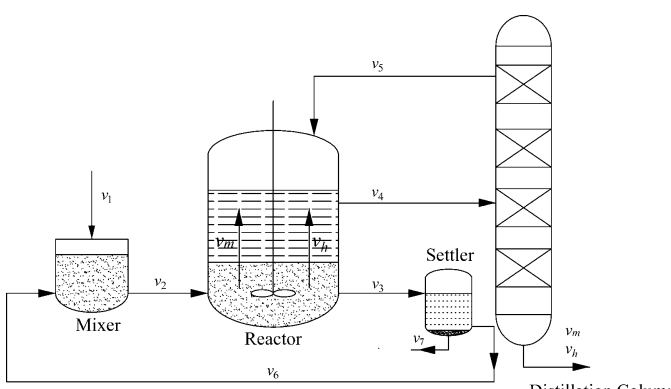


Fig. 2. Diagram of the combined process of cellulose degradation and product separation.

3.2. Continuous model

Coupling reaction with a separation unit in an integrated reactor has the potential for enhancing the conversion and selectivity of an equilibrium reaction, and reducing the cost of equipment [27], as is always being used in the industry. Hence, a continuous model of cellulose degradation and product separation in an integrated reactor is proposed based on the above reaction mechanism and process analysis. Fig. 2 shows the schematic flowsheet of this process. The cellulose particles at a rate of v_1 are well mixed with the reflux cooperative IL pairs to form IL/cellulose slurry. The slurry is pumped into the integrated continuous stirred tank reactor (CSTR) at a rate of v_2 to conduct the depolymerization reaction. During this process, the mixture of the lower phase containing solid cellulose, products, by-products generated by the repolymerization reaction and IL pairs will be delivered to a settler at a rate of v_3 to separate solid and liquid and to recycle the ILs and other liquid contents. In the reactor, the extract phase (upper phase), which contains the value-added volatile products, is transported to a distillation column to separate the extractant and products at a rate of v_4 . The parameter v_5 is the flow rate of recycled pure extractant, v_6 is the rate of recycled ILs, v_7 is the unreactive cellulose rate, and v_8 is the rate of pure products. Parameters v_m and v_h are rates of pure methanol-soluble and hexane-soluble products transferring from the IL phase to the extract phase.

Just as in most biomass-based processes, the lack of correlative experimental data and precise physical and chemical properties is the main obstacles to the proper model exploration. Here are some hypotheses that we propose to simplify the simulation, based on the experimental data and theoretic analysis.

1. No cellulose particles exist in the extract.
2. When the extract flow rate v_4 is ten times higher than cellulose feeding rate, the product distribution coefficient R_1 and R_2 equal 0.5 and 1.0, respectively. And the rate of mass transfer is not taken into account.
3. The unreacted cellulose settles in the settler entirely.
4. The operation is under steady-state condition.
5. The reactive cellulose concentration in the CSTR remains constant and it equals the saturated concentration.

In this system, steady-state operation makes sure that the cellulose concentration does not change with time. Then, Eqs. (13)–(14) give the two parts of cellulose concentration in the CSTR under steady-state condition.

$$c_{rf} = \frac{(1 - \Phi)S\rho_{IL}}{100} \quad (13)$$

$$c_{rs} = \frac{\Phi S \rho_{IL}}{100} \quad (14)$$

In above expressions, only Φ changes with temperature while the concentration of active cellulose is constant at a certain temperature. Because the reactant concentration does not change in this continuous process, the kinetic expression under the steady-state operation should be modified from Eq. (9) and (10) and is given as Eqs. (15)–(16).

$$k'_f c_{rf} + k'_s c_{rs} - k'_1 c_m + k'_{-1} c_h - R_1 \frac{v_4}{\rho_4} \frac{c_m}{V_{IL}} = 0 \quad (15)$$

$$k'_1 c_m - k'_{-1} c_h - R_2 \frac{v_4}{\rho_4} \frac{c_h}{V_{IL}} = 0 \quad (16)$$

V_{IL} is the volume of IL pairs in the reactor, ρ_i is the density of each flow i ($i = 1$ –8). R_1 is the distribution coefficient of methanol-soluble products and R_2 is the distribution coefficient of hexane-soluble products, expressed by

$$R_1 = \frac{c_m^E}{c_m} \quad (17)$$

$$R_2 = \frac{c_h^E}{c_h} \quad (18)$$

where c_m^E and c_h^E are the methanol-soluble and hexane-soluble products concentration in the extract phase.

The mass balance in the whole system, mixer, reactor, settler and distillation column yields the relations

$$v_1 = v_8 + v_7 \quad (19)$$

$$v_1 + v_6 = v_2 \quad (20)$$

$$v_2 + v_5 = v_4 + v_3 \quad (21)$$

$$v_6 + v_7 = v_3 \quad (22)$$

$$v_4 = v_5 + v_8 \quad (23)$$

Apart from the mass balance equations mentioned above, there are some equations relating to the concentration and flow rate by considering the mass conservation of each species. Following equations show the flow rate of pure methanol-soluble and hexane-soluble products transferring to the extract phase.

$$v_m = \frac{v_4}{\rho_4} c_m^E \quad (24)$$

$$v_h = \frac{v_4}{\rho_4} c_h^E \quad (25)$$

By comparing the Eqs. (15)–(20) with Eqs. (24)–(25), we can get Eq. (26) and deduce the following density relation by assuming those three liquids being idea liquid, Eq. (27). The others flow density can also be calculate using this method.

$$v_8 = v_m + v_h \quad (26)$$

$$\frac{1}{\rho_8} = \frac{v_m}{v_8 \rho_m} + \frac{v_h}{v_8 \rho_h} \quad (27)$$

There is a characteristic equation to describe the relation between the volume of IL pairs in the reactor and the rate of feeding, Eq. (28). And the conversion of cellulose can be described as Eqs. (29)–(30).

$$V_{IL} = \frac{v_2}{\rho_2} t_R \quad (28)$$

$$V_{IL} = \frac{c_0 v_2}{(-r_c) \rho_2} X \quad (29)$$

$$X = \frac{v_8}{v_1} \quad (30)$$

Table 1

Determined rate constants of cellulose degradation in cooperative ILs at various temperatures.

Temperature (K)	Rate constant (s^{-1})			
	k'_f	k'_s	k'_1	k'_{-1}
433	2.88×10^{-3}	2.96×10^{-6}	2.93×10^{-2}	8.84×10^{-3}
453	3.22×10^{-3}	1.09×10^{-5}	1.72×10^{-1}	4.06×10^{-2}
473	1.15×10^{-2}	1.30×10^{-5}	1.73×10^{-1}	3.93×10^{-2}

where t_R is the average retention time of feedstock, and X and r_c are the conversion and degradation rate of cellulose. Eqs. (15)–(30) have a general description of the continuous operation in the integrated CSTR, and those relative equations were solved by programming with the software package Matlab to get a clear recognition of the continuous process.

4. Results and discussion

4.1. Kinetic study in batch reactor

4.1.1. Kinetic parameters estimation in batch reactor

The kinetic constants were estimated by the experimental data exclusively considering the final reaction chemical equilibrium using the optimizing program in Matlab. The obtained constants at different temperatures are summarized in Table 1 when the acid IL $C_4H_8SO_3HmimHSO_4$ is used as the cellulose degradation catalyst. As shown in Table 1, the value of k_f is far higher than that of k_s (more than 10^3 times) in each case, which is similar to the ratio that recently reported [25], indicating that the content of the fast-reaction cellulose is crucial in this cooperative IL pairs system. This result also explains well with our previous studies, where amorphous cellulose and natural cellulose in lignocellulosic biomass are more flexible than the microcrystal cellulose for degradation [21,22], because of lower crystallinity and more fast-reaction content there. Table 1 demonstrates that the reaction constants of the cellulose degradation to intermediate (methanol-soluble fraction) are significantly influenced by the reaction temperature. And an obvious increase is shown when the reaction temperature is elevated from 453 to 473 K, which suggests the sharp disappearance of the residual solid (unreacted feed) in the cooperative IL pairs at 473 K [21] where the degradation of cellulose in the presence of cooperative IL pairs is a continuous process of cellulose depolymerization to methanol soluble fraction and then the degradation of the intermediate (methanol soluble fraction) to the hexane soluble chemical (the final products). Table 1 also shows that the reaction rate constant of cellulose depolymerization (k_f) is far less than that of hexane-soluble products (k_1) under various reaction temperatures during this two-step continuous process. It also implies that the heterogenetic reaction of cellulose particles to methanol-soluble compounds by cooperative IL pairs is the rate-controlling step as analyzed before [21–23].

The changes of cellulose and product concentration under various reaction temperatures are also simulated using Matlab. The initial cellulose concentration (c_0) is designated to be 200 g/L according to the feed cellulose ratio in the cooperative IL pairs reported in [21]. The solubility of cellulose in ILs is set to 12 g/100 g [3]. As shown in Fig. 3, the reaction temperature has a significant effect on the cellulose degradation. For example, nearly 50% of the cellulose is converted when it is treated at 433 K for 1500 s. However, when the reaction temperature is elevated to 473 K, 100% cellulose can be converted with more than 80% of the hexane-soluble fraction selectivity during 500 s. These results are fitted well with our previous experimental results [21], where cellulose can be converted 100% in 15 min. Fig. 4 further demonstrates that the species of the cellulose are also a key factor for

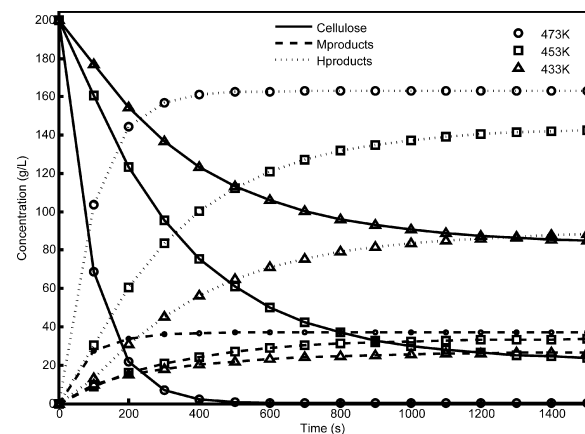


Fig. 3. Concentration–time profiles of cellulose to methanol-soluble and hexane-soluble products at different temperatures in the batch reactor.

cellulose depolymerization. As shown in Fig. 4, the fast-reaction cellulose fragment suffers a sharp depolymerisation at each case, whereas, the concentration of the slow-reaction fraction has no significant change. Therefore, the high content of the refractory slow-reaction cellulose at 433 K (measured according to Eq. (8)) is considered to be responsible for its low conversion. And the high concentration of slow-reaction fragment significantly hinders its efficient utilization, which is also a main reason for the fact that many investigations focus on the cellulose pretreatment [2].

4.1.2. Catalyst effect

Fig. 5 shows the variation of cellulose and product concentration in the batch reactor with time under three different catalysis conditions ($C_4H_8SO_3HmimHSO_4$, H_2SO_4 and no catalyst) base on the optimized kinetic parameters obtained from Matlab. As shown in Fig. 5, the conversion rate of cellulose without any catalyst is far away from the catalytic system and with less cellulose conversion and product formation. The acid IL $C_4H_8SO_3HmimHSO_4$ is the most efficient catalyst in this system for cellulose degradation, and the cellulose reach a complete degradation at 500 s. However, when H_2SO_4 is used as catalyst, just 72.4% of the cellulose degradation is attained at the time. Considering that the acid IL has higher catalytic effect than mineral acid and less corrosion of the equipment, $C_4H_8SO_3HmimHSO_4$ is adopted for the modeling of cellulose catalytic degradation in the integrated CSTR.

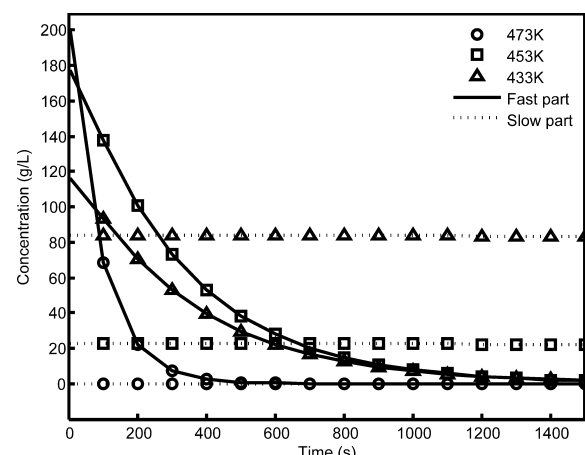


Fig. 4. Concentration–time profiles of the fast-reaction and slow-reaction cellulose in the batch reactor at various temperatures.

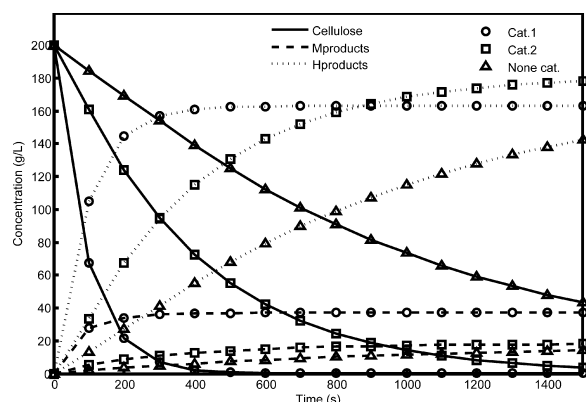


Fig. 5. Concentration–time profiles of cellulose to methanol-soluble and hexane-soluble products by different catalyst in the batch reactor.

Table 2
Simulation parameters for integrated CSTR model.

No.	Parameter	Value	Ref.
1	ρ_{IL}	1000	[28]
2	ρ_1	1500	[29]
3	ρ_5	690	[30]
4	ρ_7	1500	[29]
5	ρ_m	1050	–
6	ρ_h	850	–
7	V_1	100	–
8	V_{IL}	70	–

4.2. Integrated CSTR studies

Based on the results from the batch reactor model (Table 1, Figs. 3 and 4), the simulation of the integrated CSTR was carried out. It should be noted that this simulation is more complex than that of the batch reaction. Therefore, in this study, only some important parameters such as reaction temperature, retention time, extract flow rate and distribution coefficient are considered and taken as variables to verify their effect on the cellulose conversion and product distribution in the integrated CSTR, while other parameters such as solubility, density of ILs, extractant, cellulose and the product are assumed as constant. Table 2 gives the simulation parameters used in the model.

4.2.1. Effect of temperature

Table 3 shows the effect of the reaction temperature on the cellulose degradation in the integrated CSTR. In this section, the feed rate of cellulose (v_1 , g/s) and the volume of ILs (V_{IL} , L) are designated as constants (Table 2). However, the value of v_6 should be less than $100 v_1/S$ as the cellulose in ILs should maintain its saturation concentration in the CSTR, where $S(g)$ represents the solubility of cellulose in 100 g IL, therefore, v_6 with the value of $100 v_1/1.2S$ is designed with the assumption that 20% of excessive cellulose is added. According to our hypotheses 2, the flow rate of reaction mixture sent to the distillation column (v_4) is designated ten times that of the feed cellulose (v_1) in order to maintain a steady-state

Table 3
Product concentrations and cellulose conversion at various temperatures^a.

Temperature (K)	Product concentration (g/L)		X (wt%)
	c_m	c_h	
433	6.5	6.5	14.1
453	5.0	14.1	24.0
473	19.9	57.9	96.4

^a $v_1 = 100$ g/s, $V_{IL} = 70$ L.

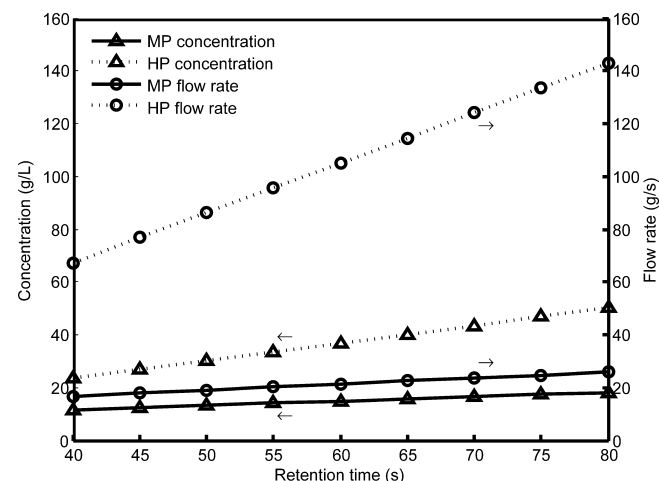


Fig. 6. Product concentration and flow rate profile of the methanol-soluble and hexane-soluble products at various retention time.

condition. The continuous simulation result shows that cellulose conversion and the product distribution are significantly affected by the thermal effect (Table 3). For example, cellulose conversion increases from 14.1% to 24.0% when the reaction temperature increases from 433 to 453 K, further increasing the temperature to 473 K will enhance the liquefaction of cellulose sharply to 96.4% conversion. It implies that the relationship between the conversion of cellulose and the reaction temperature is exponential to some extent. In this process, reaction temperature plays an important role in the conversion of cellulose, and there are some key factors that will push the transformation process forward intensively at relatively higher temperature, for example, the dissolution cellulose in ILs, the nonvolatile products in methanol and volatile products in hexane, and the endotherm of depolymerization reaction will also take effect on this conversion. Except for the higher reaction rate constant at high temperature, this phenomenon is also greatly caused by the higher content of the fast-reaction cellulose at elevated temperature, because this fragment is more ready to be converted (Table 1 and Fig. 4). Moreover, with the increase of the temperature, the ratio of hexane-soluble to methanol-soluble products is also increased, which means that the more hexane-soluble products will be yielded at a high temperature. This well fits with the simulated results of the kinetic parameters in Table 1 that the value of k_1 has a more obvious increasing than that of k_{-1} . Then, the following analysis is based on the simulated result achieved at 473 K because the small molecular weight product in the hexane-soluble part is preferable.

4.2.2. Effect of retention time

In this model, it is assumed that the feeding rate maintains constant and reactive cellulose concentration is saturate in the ILs when this process is under the steady state. The cellulose conversion is linearly related to the average retention time according to Eqs. (28)–(29). In this section, the feeding rate v_1 is set to 200 g/L, due to the high reaction rate under 473 K. It can be calculated that the cellulose conversion increases from 42.1% to 84.4% linearly, when the retention time changes from 40 to 80 s. Fig. 6 shows the change of product concentration and flow rate with the retention time. It can be seen from Fig. 6 that the four parameters are increased linearly with the retention time, and among these, the flow rate of hexane-soluble product increases fastest. Those calculated results illustrate that increasing the retention time has a positive effect on the product yielding. On the other hand, longer retention time means bigger reactor volume, resulting in

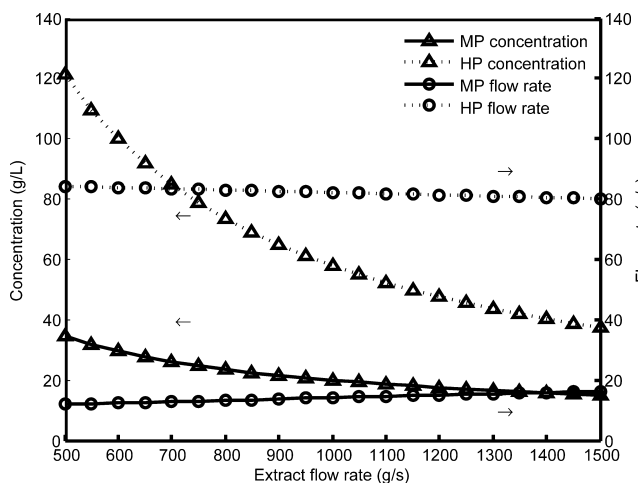


Fig. 7. Product concentration and flow rate profile of the methanol-soluble and hexane-soluble products at various extract flow rates.

increasing of equipment cost. Therefore, the appropriate value of retention time should be determined through optimization.

4.2.3. Effects of extract flow rate

Fig. 7 shows the effect of the extract flow rate v_4 on the product distribution, when the parameters of V_{IL} , T , and v_1 are set to 70 L, 473 K and 100 g/s, respectively. As shown in Fig. 7, with the increase of the extract flow rate (v_4), the flow rate of hexane-soluble products (v_h) has a small decrease and methanol-soluble products (v_m) has a corresponding increase. However, the concentrations of products both in methanol and hexane (c_m , c_h) decrease sharply. Especially, when the extract flow rate increases from 500 to 1500 g/s, the hexane-soluble product decreases sharply from 121.3 to 27.4 g/L. Therefore, we can safely conclude that the hexane-soluble products are more sensitive than that of methanol-soluble fraction. Although the operation purpose is to get more hexane-soluble product, the energy consumption should be taken into account. Much lower concentration of products in the extract phase will undoubtedly result in an increased cost for the separation of products and extractant. It illustrates that the appropriate value of extract flow needs more calculation by comprehensive consideration of the product yield and energy consumption before it is decided.

4.2.4. Effects of distribution coefficients

In this model, the distribution coefficients R_1 , R_2 are assumed, due to the lack of precise mass transfer parameters at high temperature. But the mass transfer plays an important role on this process, caused by its effect on the product distribution in the two phases in fact. Table 4 shows the effect of R_1 value on the product distribution while R_2 remains 1.0, and the effect of R_2 value on the product distribution while R_1 remains 0.5. When the value of R_1

Table 4

Product concentration and flow rate at various distribution coefficients^a.

Distribution coefficient		Concentration (g/L) and flow rate (g/s)			
R_1	R_2	c_m	c_h	v_m	v_h
0.3	1.0	21.2	61.5	9.0	87.4
0.5	1.0	19.9	57.9	14.1	82.2
0.7	1.0	18.8	54.7	18.7	77.7
0.5	0.5	30.2	105.7	21.4	75.0
0.5	0.7	24.5	79.5	17.4	79.0
0.5	1.0	19.9	57.9	14.1	82.2

^a $v_1 = 100$ g/s, $V_{IL} = 70$ L, $T = 473$ K.

rises from 0.3 to 0.7, the mass flow rate of hexane-soluble products v_h decreases from 87.4 to 77.7 g/s. Hence, the smaller value of R_1 is desirable since the total mass rate of products is not changed. The mass flow rate of hexane-soluble products v_h increases from 75.0 to 82.2 g/s when the value of R_2 increases from 0.5 to 1.0. This increase is important from the view point of industry as much high concentration of the final products in the reaction phase goes against the depolymerisation process and repolymerization will always take place between the products. Therefore, it is important to use an extractant that has a high value of R_2 and a much small R_1 .

5. Conclusion

In this work, a kinetic model was firstly proposed to describe the catalytic degradation of cellulose over cooperative ionic liquids in a batch reactor in view of the experimental data and the final reaction chemical equilibrium. Then, a mathematical model including simultaneous cellulose catalytic degradation and product separation has been built for the integrated CSTR based on the kinetic model in the batch reactor. The simulation result shows that reaction temperature, retention time, extract flow rate, and the distribution coefficient are all crucial for cellulose degradation. The first two factors mainly affect the cellulose conversion, in which relatively high temperature and larger retention time are favorable in the cellulose conversion. The extract flow rate and distribution coefficient have a more significant effect on the product concentration, with a higher hexane-soluble product distribution coefficient and lower extract flow rate resulting in higher concentrations of the products. These simulation results should shed light on better understanding the catalytic conversion of cellulose in ionic liquid pairs and forecasting the product distribution in a continuous operation for the industrial transformation of biomass.

Acknowledgments

The authors gratefully acknowledge financial support of the Natural Science Foundation of China (Grants 21336002, 21276094, and 51306191), the Doctoral Fund of the Ministry of Education of China (Grant 20130172110043), and the Natural Science Foundation of Guangdong Province, China.

References

- [1] M.E. Himmel, S.-Y. Ding, D.K. Johnson, W.S. Adney, M.R. Nimlos, J.W. Brady, T.D. Foust, *Science* 315 (2007) 804–807.
- [2] Q. Zhang, F. Jerome, *ChemSusChem* 6 (2013) 2042–2044.
- [3] A. Brandt, J. Gräsvik, J.P. Hallett, T. Welton, *Green Chem.* 15 (2013) 550–583.
- [4] J. Long, B. Guo, J. Teng, Y. Yu, L. Wang, X. Li, *Bioresour. Technol.* 102 (2011) 10114–10123.
- [5] P. Biller, A.B. Ross, *Bioresour. Technol.* 102 (2011) 215–225.
- [6] R. Harun, M.K. Danquah, G.M. Forde, *J. Chem. Technol. Biotechnol.* 85 (2009) 199–203.
- [7] A.F. Lee, K. Wilson, *Catal. Today* 242 (2015) 3–18.
- [8] N. Ji, T. Zhang, M. Zheng, A. Wang, H. Wang, X. Wang, J.G. Chen, *Angew. Chem. Int. Ed.* 120 (2008) 8638–8641.
- [9] Q. Gan, S.J. Allen, G. Taylor, *J. Chem. Technol. Biotechnol.* 80 (2005) 688–698.
- [10] A.I. Torres, M. Tsapatsis, P. Daoutidis, *Comput. Chem. Eng.* 42 (2012) 130–137.
- [11] M. Goto, J.M. Smith, B.J. McCoy, *Ind. Eng. Chem. Res.* 29 (1990) 282–289.
- [12] R.P. Swatloski, S.K. Spear, J.D. Holbrey, R.D. Rogers, *J. Am. Chem. Soc.* 124 (2002) 4974–4975.
- [13] J.B. Binder, M.J. Gray, J.F. White, Z.C. Zhang, J.E. Holladay, *Biomass Bioenerg.* 33 (2009) 1122–1130.
- [14] H. Xie, S. Li, S. Zhang, *Green Chem.* 7 (2005) 606–608.
- [15] S. Hyvarinen, J.P. Mikkola, D.Y. Murzin, M. Vahter, M. Kaljurand, M. Koel, *Catal. Today* 223 (2014) 18–24.
- [16] W. Liu, J. Holladay, *Catal. Today* 200 (2013) 106–116.
- [17] C. Li, Z.K. Zhao, *Adv. Syn. Catal.* 349 (2007) 1847–1850.
- [18] H. Wang, G. Gurau, R.D. Rogers, *Chem. Soc. Rev.* 41 (2012) 1519–1537.
- [19] J. Long, X. Li, L. Wang, N. Zhang, *Sci. Chin. Chem.* 55 (2012) 1500–1508.
- [20] H. Zhao, J.E. Holladay, H. Brown, Z.C. Zhang, *Science* 316 (2007) 1597–1600.
- [21] J. Long, B. Guo, X. Li, Y. Jiang, F. Wang, S.C. Tsang, L. Wang, K.M.K. Yu, *Green Chem.* 13 (2011) 2334–2338.

- [22] J. Long, B. Guo, X. Li, F. Wang, L. Wang, *Acta Phys. Chim. Sin.* 27 (2011) 995–999.
- [23] J. Long, B. Guo, X. Li, F. Wang, L. Wang, *Green Chem.* 14 (2012) 1935–1941.
- [24] W. Liu, F. Zheng, J. Li, A. Cooper, *AIChE J.* 60 (2013) 300–314.
- [25] L. Chen, H. Zhang, J. Li, M. Lu, X. Guo, L. Han, *Bioresour. Technol.* 177 (2015) 8–16.
- [26] L. Yan, A.A. Greenwood, A. Hossain, B. Yang, *RSC Adv.* 4 (2014) 23492–23504.
- [27] K.D. Samant, K.M. Ng, *AIChE J.* 44 (1998) 2212–2228.
- [28] H. Machida, R. Taguchi, Y. Sato, R.L. Smith Jr., *J. Chem. Eng. Data* 56 (2011) 923–928.
- [29] C. Sun, *J. Pharm. Sci.* 94 (2005) 2132–2134.
- [30] K.R. Harris, *J. Chem. Soc.* 78 (1982) 2265–2274.